Tuning Silica Surface Properties for Enhanced Performance in Si–UHMWPE Battery Separators

Mohammad Abou Taha, Guillaume Sudre, Aurel Radulescu, Fabrice Gouanvé, Matthieu Fumagalli, Thomas Chaussée, Véronique Bounor-Legaré, René Fulchiron

Tuning Silica Surface Properties for Enhanced Performance in Si-UHMWPE Battery Separators

Mohammad Abou Taha[†,‡], Guillaume Sudre[†], Aurel Radulescu[§], Fabrice Gouanvé[†], Matthieu Fumagalli[†], Thomas Chaussée[‡], Véronique Bounor-Legaré[†] and René Fulchiron*[†]

[†]Universite Claude Bernard Lyon 1, INSA Lyon, Université Jean Monnet, CNRS, UMR 5223, Ingénierie des Matériaux Polymères, F-69622 Villeurbanne Cedex, France.

[‡]Solvay Silica, 15 rue Pierre Pays, F-69660 Collonges-au-Mont-d'Or, France.

[§]Jülich Centre for Neutron Science, Garching Forschungszentrum, Lichtenbergstraße 1, D-85747 Garching bei München, Germany.

*Corresponding author: rene.fulchiron@univ-lyon1.fr

Graphical Abstract:

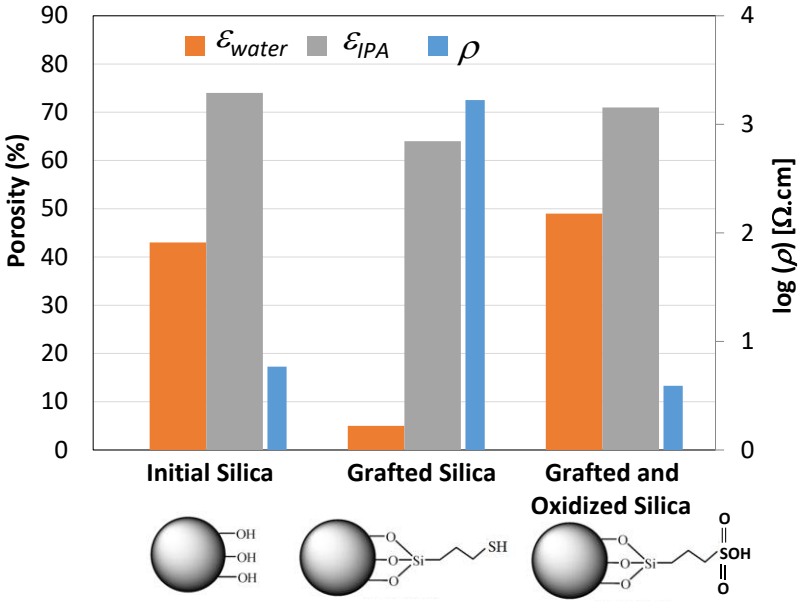

Keywords: Battery separator, UHMWPE, Silica, Hydrophobicity, Hydrophilicity

Abstract:

By chemically tuning the surface of precipitated silica, we propose an approach to vary the hydrophilicity and to elucidate its impact on the state of dispersion of silica aggregates in hydrophobic materials. Precipitated silica underwent reversible chemical modification which transformed its surface from a hydrophilic surface to a hydrophobic surface, in order to promote the interactions with hydrophobic environments, e.g., suspension of silica in hydrophobic solvents and dispersion in nanocomposites. Hence, tunable hydrophobic molecules, i.e. 3-mercaptopropyltrimethoxysilane (MPTMS) were grafted onto the surface of silica. In a first step, the properties of the surface of silica were adapted to enhance the dispersion of particles in a hydrophobic medium (e.g., processing hydrophobic polymers filled with silica). Afterwards, the obtained modified silica underwent a chemical tuning to recover a part of its initial hydrophilicity, which is desired for some applications like batteries separators. Thereby, the grafted molecules onto the surface of silica were oxidized to decrease the hydrophobicity of the grafted functions. For each surface treatment of silica particles, solid-state NMR analyses were used to confirm qualitatively the presence of the grafted molecules onto the surface of silica, TGA analysis and conductance measurements were used to quantify the grafted molecules. Water sorption isotherms were also used to characterize the hydrophilicity change of silica. Finally, the obtained silicas were used in formulations of UHMWPE (Ultra-high molecular weight polyethylene)-silica batteries separators that were characterized by scattering electron microscopy (SEM) and small angle neutron scattering (SANS), porosity measurements and electrical resistance measurements. The silica grafted and then oxidized presents the best dispersion in the UHMWPE while presenting the high hydrophilicity needed for the low resistivity of the membrane.

Introduction:

Silica particles exhibit diverse surface properties that are dependent on the synthesis process, including surface area, surface chemistry, and surface hydrophilicity. These properties can significantly impact the reactivity, structure, and physical properties when combined with other materials, such as for example mechanical reinforcement in elastomers, processability, and electrical resistivity in battery separators [1-3]. These final properties of materials are also mainly related to the concentration of the silica and to its dispersion state in the polymer matrix [4-5]. The surface of silica commonly contains various proportions of hydrophilic chemical groups, siloxane bridges Si-O-Si and silanols Si-OH [6]. The silanols are responsible for the chemical interactions and/or reactions (grafting) between silica particles and polymer chains or compounds containing a reactive function with respect to silanol. Silanols can be obtained through two processes: during the synthesis of silica and by rehydroxylation of dehydroxylated silica [7]. In order to enhance the affinity between the silica and the polymer and thus its dispersion state, silica is mainly modified with organic species. There are several methods to chemically modify the surface of silica with organic functional groups [8-9]. These methods include reaction with organoalkoxysilanes or organic molecules, and chlorination of silica surfaces followed by modification of the Si-Cl bond with a suitable reagent [10]. Here, the general trend is to give silica a level of hydrophobicity that enables good interactions with the polymer matrix and hence good dispersion. However, when applied as a battery membrane, it has been shown that this hydrophobicity becomes detrimental to electrical conductivity because a significant proportion of pores remains inaccessible to the electrolyte [11-14]. UHMWPE-silica battery separators contain over 50 vol% silica that contributes to several critical aspects of this application, such as improving oil retention that will give the final porosity, reducing shrinkage and enhancing the electrolyte wettability of the separators [15-17]. While only pure precipitated and fumed silica have been used in this application to date, the objective of this work is to evaluate the effects of different surface treatments on different types of precipitated silica and to explore the potential for tuning the silica surface properties during the separator production process and in its final application in the battery. Thereafter, this paper will focus specifically on the functionalization of particles using organoalkoxysilanes via hydrolysis and condensation functionalization to improve dispersion, followed by *in situ* oxidation to remove the hydrophobicity after the membrane manufacturing and improve the conductivity. Most of the studied methods for modifying silica particles have been conducted using purely organic solvents, such as hydrocarbon-based solvents, as it was previously believed that reaction intermediates would be different in alcoholic or aqueous media [18]. However, recent studies have demonstrated the feasibility of grafting in mixed media, such as water/alcohol [19]. In this work, MPTMS was selected due to its thiol (-SH) functions, which are known to be hydrophobic in nature, and its ability to be

chemically tuned through oxidation to sulfonic acid (-SO_3H), thus restoring the hydrophilicity of the silica surface chemistry.

In the present work, the successive ways of chemically modify the silica will be shown. At the different steps, the silica will be characterized to evaluate the chemical modification and its efficiency on its water sorption. Then the different silica will be blended with oil and UHMWPE to manufacture membranes that will be analyzed in terms of morphology, porosity and electrical resistivity as battery separators.

I) Materials and reagents

Porous precipitated silica was supplied from the R&I Silica Solvay laboratory. A specific silica 19AESR010® was used. It has a specific surface area of 213 $m^2.g^{-1}$, high dioctyl adipate oil absorption capacity (DOA) of 221 $mL.100\ g^{-1}$, high content of isolated hydroxyls 2.85 $mmol.g^{-1}$ and is qualified as hydrophilic by its supplier. The particles form agglomerates of D_{50} around 6 µm. This silica was used because its characteristics because, a priori, the grafting could be more efficient owing to the high specific surface area.

The used alkoxysilane is 3-mercaptopropyltrimethoxysilane $HS(CH_2)_3Si(OCH_3)_3$ (MPTMS, 95%) was purchased from Sigma-Aldrich. With a molar mass of 196.34 $g.mol^{-1}$, its boiling point is around 213 – 215 °C.

The ultra-high molecular weight polyethylene (UHMWPE) is the GUR4150® produced and supplied by Celanese. It is a white powder with a melting temperature of 135°C (taken at the onset of the peak measured by DSC at 20°C/min [21]), a density of 0.93 $g.cm^{-3}$ and a volume resistivity of 10^{12} Ω.m. It has a reported viscosimetric molar mass over 9 000 000 $g.mol^{-1}$ [20].

Nytex 820® oil is a naphthenic oil (plasticizer) produced by Nynas and composed of heavy naphthenic hydrotreated distillates. It has an initial boiling point higher than 250 °C and has thermal stability up to 280 °C. Its glass transition is at -64°C. Moreover, it has a viscosity of about 2.2×10^{-3} Pa.s at 165°C and has a density of 0.91 $g.cm^{-3}$. It is reported that Nytex 820® is a solvent of polyethylene at high temperatures [20-21].

The isopropyl alcohol (IPA) of 98% of purity used for Soxhlet extraction of process oil in the membranes and porosity measurements was provided by Sigma-Aldrich. Anhydrous toluene (99.8% purity) to perform the silica grafting, hydrogen peroxide solution (34.5-36.5%) to perform the oxidations reactions and sodium hydroxide solution (0.01 M) to carry out the conductometry titration were also all provided by Sigma-Aldrich.

II) Silica modification

Silica underwent successive chemical modifications in order to:

i) transform its surface from a super hydrophilic surface to hydrophobic, taking advantage of the methoxysilane groups of MPTMS that can condense on the silica surface with the silanols and the thiol alkyl chain ends that would increase the hydrophobicity.

ii) recover hydrophilicity, which is desired for the battery separator application through the oxidization reaction of the thiol group of the grafted molecule.

1. Alkoxysilane grafting onto the silica particles:

For this first type of modification, the followed protocol for grafting silica with alkoxysilane is inspired from one of our previous study, [22] in which a mass grafting yield of approximately 2-3 wt% was obtained. For the condensation reaction, we consider that a mechanism of alkoxylation happens during the condensation where an alcohol molecule is eliminated to form “oxo” bridges or, in the silicon case, “siloxane” bridges (Si-O-Si) [18] as shown in Figure 1.

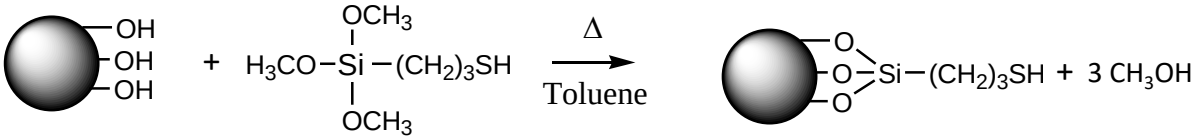

Figure 1: Reactional scheme of the MPTMS grafting onto silica

A mass of 10 g of silica was dispersed in 250 mL of anhydrous toluene for 60 min under vigorous mechanical stirring (in reflux). Next, alkoxysilane was added to the suspension with a mass ratio of 2:1 of silica: MPTMS, and the reactional medium was treated for 48 h at 80 °C. Then, toluene was evaporated, and modified silica particles were dried in a vacuum oven at 90 °C for 12 h. To eliminate unreacted alkoxysilane, Soxhlet extraction was carried out for 72 h with IPA, and finally, the residue was dried in a vacuum oven at 90°C for 12 h. This silica is called grafted silica in the discussion.

2. Chemical tuning of the grafted molecules:

The grafted silica was oxidized by hydrogen peroxide following the scheme given in Figure 2 adapted from the publication of Bayse [23]. For this, the grafted silica particles were put in a solution of 38 % of hydrogen peroxide under stirring for 72 hours. The suspension was centrifuged at low temperature (15 °C), and the solid has been washed 4 - 5 times with deionized water (centrifuged and separated from water until measuring a neutral pH). The obtained silica called grafted-oxidized was dried overnight at 80 °C.

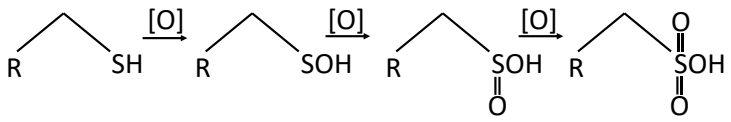

Figure 2: Oxidation reactions of the thiol group to form sulfonic acid

3. Characterization of silica particles:

a) Solid-State NMR

Solid-state ^{13}C and ^{29}Si NMR was directly performed on silica powder using a Brüker Avance WB 500 MHz spectrometer equipped with a 4 mm MAS probe. A cross polarization sequence was used since it is sensitive to the ^{1}H-^{29}Si dipole coupling. This sequence consists of transferring part of the magnetization from the abundant spins (^{1}H) to the rare spins (^{29}Si) via the ^{1}H-^{29}Si dipole interaction during a chosen contact time.

b) Thermogravimetric Analysis (TGA)

The TGA measurements were carried out on a TA Instruments Q500 thermogravimetric analyzer with a ramp of 10°C.min^{-1} from ambient temperature to 900°C, in a helium flow of 40 mL.min^{-1}.

c) Conductometry titration

Sodium hydroxide solution (0.01 M) was used to determine the concentration of sulfonic acid groups. The conductance was measured during titration using a Tacussel conductometer with a probe. First, around 0.5 g of silica was suspended in deionized water and stirred for 5 min before starting the titration coupled with the conductance measurement.

d) Dynamic vapor sorption analyzer (DVS)

Dynamic vapor sorption analyzer, DVS Advantage (Surface Measurement Systems Ltd., London, UK), was used to determine the water sorption isotherms of the silica powder. The vapor partial pressure (P) was controlled by mixing dry and saturated nitrogen, using electronic mass flow controllers. The experiments were carried out at 25°C for water vapor activities, a_w, ranging from 0.1 to 0.9. The initial mass of the samples was approximately 50 mg. The samples were pre-dried in the analyzer using dry nitrogen to obtain the mass of the dry powder. The partial pressure of water was established within the apparatus and the mass uptake was followed as a function of time. The equilibrium was considered to be reached when the mass change in time became practically null ($\mathrm{d}m/\mathrm{d}t < 2 \times 10^{-4}$ mg.min^{-1}) for 5 consecutive minutes. Afterward, the water activity was increased automatically to the target. The isotherm sorption of water describes the relationship between the concentration of water in the powder and water activity. The water activity a_w is the ratio of the pressure of water in equilibrium

with the material (P) and the saturated vapor pressure of pure water (P_{sat}) at the same temperature, as seen in Eq 1:

$$a_w = \frac{P}{P_{sat}} = \frac{H}{100} \qquad \textbf{Eq 1}$$

where H is the relative humidity (%) at equilibrium.

III) Si-UHMWPE membranes

1. Protocol of preparation

The used technique is referred to as the thermally induced phase separation (TIPS) [24] and has also been the subject of several works to prepare microporous polymer membranes using different polymers such as PE [25-26], polypropylene [27-28], polyvinyl fluoride [29-30], polystyrene [31] and others [32]. It can be pointed out that in the membranes based on UHMWPE, this polymer provides good mechanical properties (wear resistance, impact strength, puncture, tensile strength. All of the mechanical properties are major assets for the production of durable batteries separators. One of the most important mechanical properties is the puncture resistance and the weight ratio Silica/UHMWPE (Si/PE) has a strong impact on this puncture resistance of the separator. When the Si/PE ratio increases, the mechanical properties of the membrane decrease [15]. Our experiences (not presented here) with a silica close to 19AESR010 gave a puncture resistance of 75% (with SI/PE of 2.5) and 66% (with Si/PE 4) compared to this of the UHMWPE without silica. Furthermore, in previous studies the variation of the composition was tested (with different silicas) and the conclusion was that increasing the quantity of silica over a ratio SI/PE of 2.5 did not improve the electrical conductivity of the membranes anymore, the maximum wettability in the membrane pores being obtained [11, 21]. Thus, in the present work, the composition was fixed.

In this study, silica, UHMWPE, and 60 wt% of process oil (the 40 % left are added in the next step of the process) were mixed slowly at room temperature using a mortar and pestle until the absorption of the oil by silica particles and the obtaining of a dry blend with the appearance of “corn-starch”. The formulations were prepared using a 76 cm^3 batch internal mixer Haake Rheomix OS equipped with counter-rotating Banbury rotors at a mixing speed of 200 rpm at 165 °C and a typical 70 - 75 % filling factor for all blends. First, the dry blend is fed in the internal mixer and then, the remaining 40 wt% of the total process oil amount of the recipe is added after approximately 2 min. This leads to a decrease of the torque of the mixer due to a lubrication effect. Finally, after a certain mixing time corresponding to the homogenization of the blend (around 7 min), the torque is stabilized. The total time of mixing was fixed to 10 min to keep the same operational conditions for all blends. The cooling of the mixture induces the phase separation and creates the porosity in the membrane.

The formulations were prepared with fixed mass ratios of Si/PE = 2.5 and oil/PE = 7.5 as displayed in Table 1 (Si/PE and oil/PE mean respectively the ratios by weight between silica and UHMWPE and process oil and UHMWPE).

Table 1: Recipes for membranes with Si/PE= 2.5 and oil/PE=7.5. The 3 types of silica have been considered (Initial, Grafted and Grafted-Oxidized)

	UHMWPE	Silica	Oil
Introduced mass (g)	5.5	13.75	41.25
wt % (introduced)	9.10	22.70	68.20
ϕ % (introduced)	10.25	11.25	78.50
wt % (post-extraction)*	28.60	71.40	(< 1)
ϕ % (post-extraction)**	47.50	52.50	

*All of quantity of process oil is extracted in the Soxhlet.
**The porous ϕ % was not considered in the calculation; it would be equal theoretically to the volume occupied by the process oil before extraction.

It must be added that, for further characterization, one formulation with initial silica was elaborated with a higher silica concentration that corresponds to Si/PE = 4.

To complete the membrane preparation, around 6 g of each blend were used to obtain a film of 15 cm × 15 cm and 250 μm of thickness by compression (press type: Servitec Polystat 200 T). The molding was made at 165°C applying first a force of 5 kN for 2 min, then a force of 125 kN for 2 min. The force was then released for a few seconds and applied again to degas the sample and avoid the heterogeneities. The films were then cooled at room temperature in the mold. Subsequently, oil extraction with IPA was carried out on the membranes using a Soxhlet for 12 h (83 °C). According to a previous study [11], after this step, there was less than 1 wt% oil in the membranes. Hence porous UHMWPE-Si separators were obtained with the composition given in Table 1. For each type of silica, at least 3 membranes have been manufactured for controlling the repeatability of the further electrical resistivity measurements. The obtained thicknesses were between 0.22 and 0.48 mm. The thickness measurements were done in five points of each membranes revealing a standard deviation of 10 %.

2. Characterization of Si-UHMWPE membranes

a) Scanning Electron Microscopy

Scanning electron microscopy (SEM) observations were carried using the Zeiss Merlin electron microscope at the Centre Technologique des Microstructures (CTμ, Universite Claude Bernard Lyon 1, Villeurbanne, France). Membrane samples were cryofractured and then placed on sample holders. Then, samples were sputter-coated with a 10 nm layer of carbon in order to limit static charging. The aim of using SEM is to qualitatively estimate the characteristic lengths of aggregates of silica, polyethylene fibrils, and pores. Also, energy-dispersive X-ray spectroscopy (EDX) was used for the

elemental analysis or chemical characterization of samples with grafted silica that are reported in supporting information.

b) Small-Angle Neutron Scattering

Small-Angle Neutron Scattering (SANS) experiments were performed at Heinz Maier-Leibnitz Zentrum (MLZ - Garching, Germany) on the KWS-2 beamline. KWS-2 is a classical pinhole SANS instrument where, combining the pinhole mode using different neutron wavelengths (λ) and sample-to-detector distances (large q: λ = 5 Å, D = 2 m; middle q: λ = 5 Å, D = 4 m; small q: λ = 10 Å, D = 20 m; $\Delta\lambda/\lambda$ = 0.1) [34]. For the present experiments, the range of scattering wavevector $q = 4\pi\lambda^{-1} \sin(\theta/2)$, θ being the scattering angle, was between 1.35×10^{-3} and 4.0×10^{-1} Å^{-1}. To characterize silica aggregates (scattering length density, $SLD_{SiO2} = 3.475 \times 10^{10}$ cm^{-2}) in the membrane, it was necessary that the rest of the sample had the same SLD. Hence, we immersed the membranes in hydrogenated IPA ($SLD_{h\text{-}IPA} = -0.39 \times 10^{10}$ cm^{-2}), which contrast-matches polyethylene ($SLD_{PE} = -0.34 \times 10^{10}$ cm^{-2}) as illustrated in Figure 3. Therefore, after cutting the membranes in discs of 8 mm diameter, they were immersed in the h-IPA for a few minutes and then put between two quartz windows with an excess of the adequate solvent before sealing. The scattering data were azimuthally averaged and corrected for background and parasitic scattering, detector sensitivity, scattering signal of the empty cell. The intensity was calibrated to absolute scale (cm^{-1}) by taking into account the sample transmission and thickness, and by using a Plexiglas secondary standard. The incoherent signal, evaluated from the pure solvent scattering, was finally subtracted.

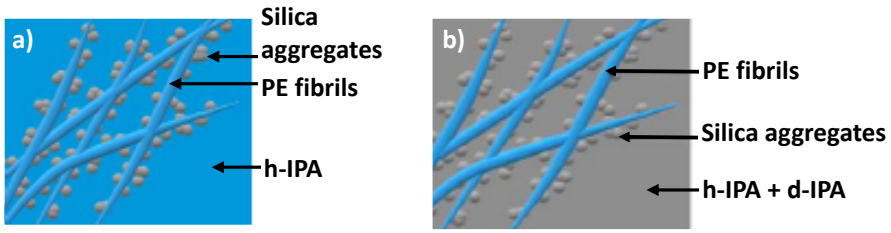

Figure 3: Contrast matching SANS experiments. a) Matching polyethylene with h-IPA, b) matching silica aggregates with a mixture of h-IPA/d-IPA.

c) Porosity using density kit

Porosity measurements were performed using a Mettler Toledo density kit combined with a ML 303T analytical balance based on the recommendation of the Battery Council International to obtain a better measurement of the volume of the membrane compared to geometrical estimation [33]. 250 µm thick square samples (1.5 cm × 1.5 cm) were dried at 80°C in an oven overnight, then each sample was weighed, and the obtained dry mass was noted W_1. For water accessible porosity measurements, each sample was immersed in boiling water for 10 min before being directly hanged in the density kit

apparatus in distilled water at room temperature. After 1 min of stabilization and after making sure to evacuate all the error-inducing air bubbles, the sample was weighed, and the submerged mass was noted W_{w2}. The sample was removed from the water, its surface was gently wiped, then the sample was weighed to obtain the saturated weight noted W_{w3}. Thus, we can calculate the water porosity ε_{water}:

$$\varepsilon_{water} = \frac{W_{w3} - W_1}{W_{w3} - W_{w2}} \qquad \textbf{Eq 2}$$

In order to access the total porosity of the membranes, IPA was used as it accesses the total porous volume of the membranes, according to Toquet et al. [11]. The IPA porosity corresponds to the total porosity obtained using mercury intrusion porosimetry. The same samples were used to obtain IPA porosity. Instead of water, IPA was filled in the density kit beaker. The dried sample was weighed submerged in IPA and W_{i2} was obtained (the mass was noted after stabilization, i.e., when no more air bubbles were seen). Then, the sample was removed from IPA, its surface was dried briskly using tissue, and it was weighed to obtain its saturated mass W_{i3}. Then, the total porosity or the IPA porosity was calculated:

$$\varepsilon_{IPA} = \frac{W_{i3} - W_1}{W_{i3} - W_{i2}} \qquad \textbf{Eq 3}$$

d) Electrical Resistivity

The electrical resistivity of membranes was measured with a mixture of sulfuric acid and water at 28°C using a Palico system, based on the recommendation of the Battery Council International (BCI) [33]. The Palico system measures separator resistance by sensing the voltage drop between two pairs of sensing electrodes in response to pulses of +100/-100 mA for 0.083 s delivered by electrodes at opposite ends of the bath. The difference in voltage drop, with and without a separator in the ionic current path, is used to calculate the separator resistance. First, the 15 cm × 15 cm square membranes were immersed in boiling water for 10 min, then in a 50/50 volume blend of sulfuric acid (d = 1.28) and water for 10 min at 27 °C. Afterward, the sample was put in the sample holder of the Palico compartment filled with the same blend of water and sulfuric acid at 28 °C. The measurement cell is a disk with a surface area (A) of 32.26 cm^2. The resistivity ρ of the sample is obtained by Eq 4. In this equation, e is the thickness of the membrane, R is the resistance measured by the Palico system, and f is a correction factor between 0.96 and 1.03 which evolves linearly as a function of the bath temperature; in our experiments, the temperature was 27.3 °C that corresponds to a correction factor of 1.015.

$$\rho = \frac{R}{e} \times f \times A$$

Eq 4

IV) Results and Discussion

1. Silica chemical modification

As described above, the silica was modified through the grafting of the MPTMS to enhance its dispersion in the UHMWPE and then oxidized to increase its final hydrophilicity for expected battery applications. First, qualitative analysis was conducted using solid-state ^{29}Si and ^{13}C NMR in order to confirm the presence of the alkoxysilane molecules onto the surface of silica.

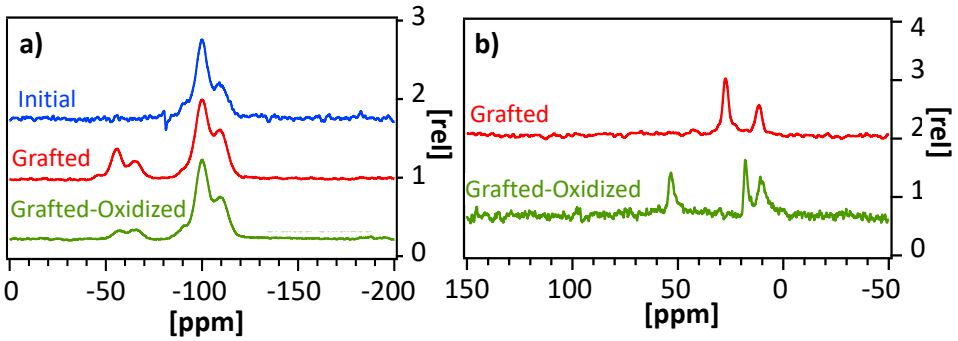

Figure 4: a): Spectra obtained from ^{29}Si solid-state NMR for initial, grafted, and grafted-oxidized silica. b): Spectra obtained from ^{13}C solid-state NMR for grafted and grafted-oxidized silica.

According to Legrand et al., several types of groups on the surface of silica can be distinguished [6] and the different silicon atoms of silica are designated by the terminology Q^n where n represents the number of bridging oxygen linked to the central atom of silicon [35]. In solid-state ^{29}Si NMR spectra of Figure 4 a, the initial silica sample presented three signals at -93, -100 and -110 ppm that correspond respectively and classically to Q^2, Q^3 and Q^4 species. Besides, on the spectra for grafted silica sample and grafted-oxidized silica sample (Figure 4 a), additional signals that correspond to T sites indicate the incorporation of organic functionalities with specific resonances (usually between -50 and -80 ppm). The T sites are detected at -57 and -66 ppm that correspond to grafted organosilicon compound, T^2 $(SiO)_2SiR$ and to T^3 species $(SiO)_3SiR$, respectively. These signals in presence of the Q^3 and Q^4 peaks confirm the grafting of the expected molecules. Furthermore, even if the analysis is not quantitative, we can notice that the intensity for the T species is lower on the spectrum corresponding to the grafted-oxidized silica compared to the one obtained for the grafted silica. This observation may evidence a decrease of the grafting amount with the oxidation protocol.

Solid-state ^{13}C NMR spectra of grafted and grafted-oxidized silica depicted also interesting results regarding the step of oxidation of MPTMS thiol function (–SH) into sulfonic acid function ($–SO_3H$). In Figure 4 b, for grafted hydrophobic silica, the signal at 27 ppm corresponds to the carbon from the bond $–\underline{C}H_2SH$. This signal is deshielded on the spectrum of the grafted and oxidized silica due to the

presence of the sulfonic acid functional group (–**C**H_2SO_3H) and is found around 50 ppm. Thus, the solid-state ^{13}C NMR analysis confirms the oxidation of the thiol group.

In order to quantify the grafting percentage, TGA analysis was conducted on the three silica samples after Soxhlet purification. As seen in Figure 5, the thermogram of grafted silica is different from the one of initial silica, proving a successful grafting of MPTMS on the silica surface. Grafted silica has a lower water content (around 50% less than initial silica) as shown by a lower mass loss in the temperature range 25 – 150 °C. For grafted-oxidized silica, water content has increased on the silica after the oxidation reaction. This is consistent with the decrease in the hydrophilicity of the grafted silica on the one hand, and of a large recovery of the hydrophilicity after oxidation, on the other hand. A grafting amount can be deduced from the weight loss in the temperature range (150 – 400 °C). However, this calculation can be a bit distorted because, at high temperature, the decomposition of the grafted molecules may be superimposed to further modification of the silica.

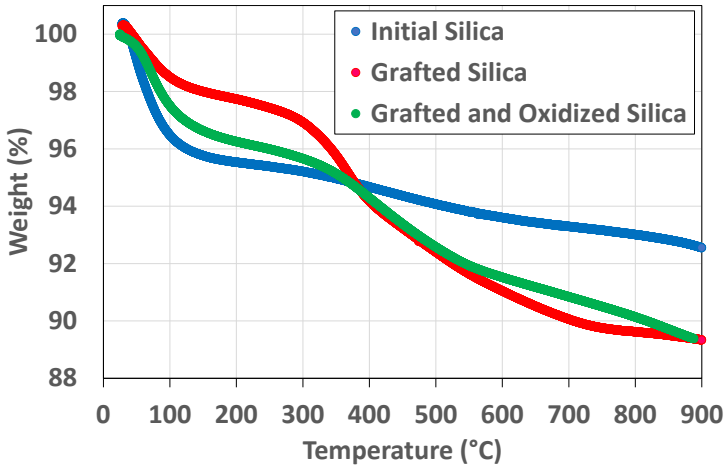

Figure 5: TGA thermograms obtained at 10°C.min^{-1} under helium for initial silica 19AESR010, silica after grafting, and grafted-oxidized silica.

In Table 2, the weight losses for different temperature ranges are displayed. Between 150 and 400 °C, the weight loss is of 3.7 wt.% for grafted silica. This value is smaller for grafted-oxidized silica (2.4 wt.%). However, the initial silica itself presents a mass loss of only 0.9 wt.% in the same temperature range. This must be considered for the quantification of MPTMS, leading to 2.8 wt.% and 1.5 wt.% of alkoxysilane derivative for grafted silica and grafted-oxidized silica, respectively.

Table 2: Calculated weight loss at different temperature ranges for analyzed silica samples.

Temperature Range	Weight Loss% initial silica	Weight Loss% grafted silica	Weight Loss% grafted-oxidized silica
30-150°C	4.4	2	3.4
150-400°C	0.9	3.7	2.4
30-900°C	7.4	10.7	10.6

In order to further quantify the grafted molecules onto the surface of silica, conductometric titration was carried out on the suspension of grafted-oxidized silica in deionized water using strong base (NaOH). From the curve in Figure 6, two break points are observed, which corresponds to a typical conductometric titration of a mixture of a strong and a weak acid by a strong base [36]. The first decrease in the conductance corresponds to the neutralization of strong acid species by the strong base as the strong acid has a high conductance value. This is due to the replacement of the fast-moving hydrogen ions H^+ by the slow-moving Na^+ ions. The electrochemical reaction at the first equivalence (V_{eq1}= 3.2 mL) is described by Eq 5:

$$SO_3H + OH^- \leftrightarrow SO_3^- + H_2O$$

Eq 5

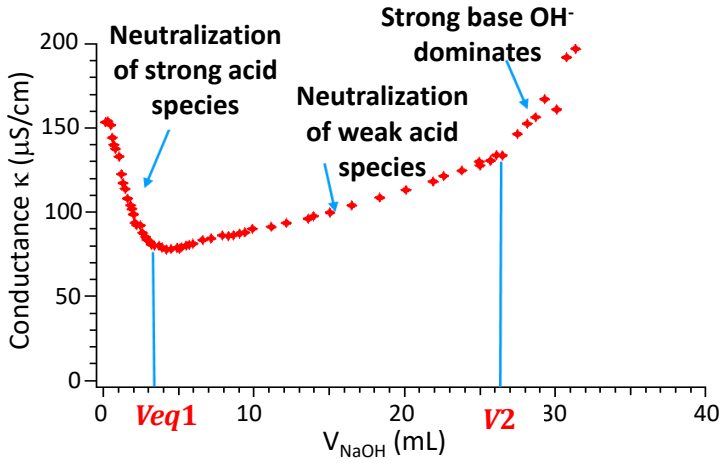

Figure 6: Conductometric titration of grafted-oxidized silica suspension (m_{Si}= 0.556 g) in water by [NaOH] = 0.01 mol.L^{-1}.

In the second part of the curve of Figure 6, a slow increase of the conductance with the added volume of sodium hydroxide base is observed, which is characteristic of the neutralization of a weak acid. The weak acid in the silica suspension can be assimilated to silanol groups that were not chemically modified by the grafting reaction [37], as well as to the small amount of the sulfinic acid (SO_2H) that has not been completely oxidized to form the strong acidic form of the species. Therefore, the increase in the second part of the curve is slower because of the formation of SO^- and SO_2^- species that have low ionic conductivity. The second breakpoint ($V2$) corresponds to the neutralization of all of the weak acid species. Beyond this breakpoint, the dominated species are the hydroxide ions OH^- (strong base) with high ionic conductivity increasing the conductance of the solution abruptly. As the strong acid is assimilated to the grafted sulfonic acid chain, thus the amount of the grafted species can be calculated using the first breakpoint (equivalence volume of NaOH) (n = [NaOH] × V_{eq1} / m_{si} = 5.8 × 10^{-5} mol.g^{-1}). Hence, a grafting of about 0.88 wt.% is calculated. Importantly, this value is calculated considering that the reactions shown in Figure 1 and Figure 2 are complete so that the obtained grafting value is the

lower limit. All things considered, this value is in accordance with the one deduced from the TGA analysis (1.5 wt.%).

The possible change of hydrophilicity has been examined by investigating the water uptake and the sorption isotherm of initial, grafted, and grafted-oxidized silica. The isothermal mass gain of water as a function of the activity (a_w), plotted in Figure 7, have the sigmoidal shape of BET II type sorption isotherms of silica. The curves obtained for the initial silica and its grafted-oxidized version have very similar water sorption isotherms. However, grafted silica depicts a lower overall water uptake and behaves differently from initial silica. The total sorption of water for the initial silica is the highest (43 %), and it is close to that of the grafted-oxidized sample (33 %) for the activity of 0.9. In contrast, the grafted silica presents the lowest mass gain (8.5 %) for the same activity. Both initial silica and grafted-oxidized silica exhibit a behavior of a hydrophilic substrate. Nevertheless, the grafted silica displays the very low capacity of adsorption of water molecules and exhibits thus a hydrophobic behavior. The oxidation of the grafted silica has permitted the recovery of the hydrophilicity of the reference silica after grafting.

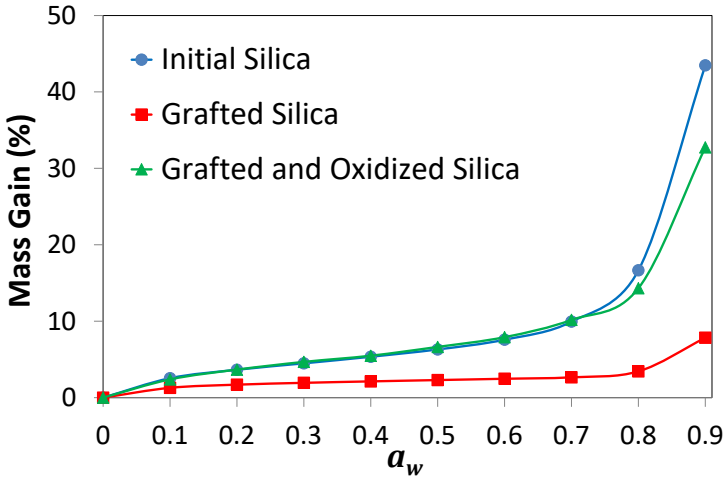

Figure 7: Water vapor sorption isotherms of initial, grafted, and grafted-oxidized silica versus water activity

2. Properties of the Si-UHMWPE membranes

Three formulations with different silica (initial, grafted, and grafted-oxidized silica) were processed in an internal mixer, and membranes were molded and oil extracted as described in the paragraph III-1. An average ratio of Si/PE= 2.5 was selected to compare the properties of the membranes. The formulations are presented in Table 1, the same amounts of polyethylene, silica, and oil were weighed as the grafted molecules on the surface of silica represent around (1 – 2 wt.%) of the total mass of silica. The only variable is the surface properties of silica in terms of hydrophilicity.

First, SEM observations were carried out to analyze the morphology of the three membranes. The obtained pictures for two magnifications are shown in Figure 8. EDX analysis has confirmed the presence of grafted molecules after the process of elaboration and extraction of membranes. These EDX data are reported in supporting information.

From these analyses, at low magnification (10 KX), SEM pictures for all types of membranes show homogeneous distribution of fibrils and torn sheets of polyethylene with dispersed silica particles. At high magnification (30 KX), it is possible to distinguish the morphologies and the silica repartition for the three different silica. Hence, a wide distribution of silica aggregates appears for membranes prepared with initial silica (with aggregates ranging between 800 to 2500 Å). On the other hand, in membranes with grafted silica and grafted-oxidized silica, silica aggregates are more dispersed, and the aggregate size seems to be slightly smaller (< 1200 Å).

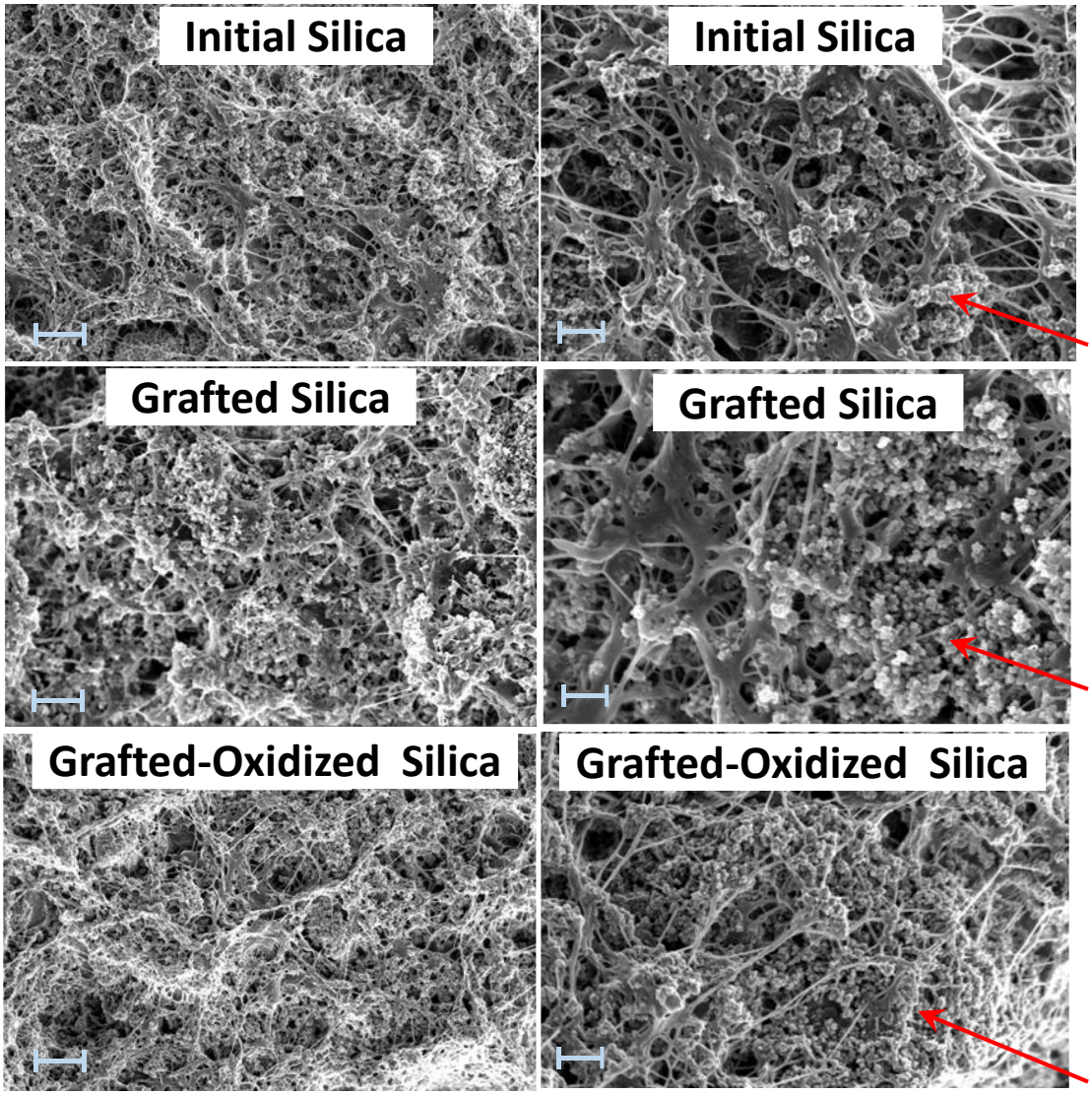

Figure 8: SEM pictures of cross-sections of the membranes at Si/PE = 2.5and oil/PE = 7.5 with the three different silica at 10 KX (left, scale bar: 1 μm) and 30 KX (right, scale bar: 300 nm). The red arrows indicate the silica domains

Nevertheless, these SEM observations are only qualitative and it is difficult to draw sound conclusions concerning the state of aggregate dispersion. To get a deeper insight on the membrane structure, small angle neutron scattering analyses were performed. This technique has been widely used in the studies of composites and for probing small, dispersed objects, for instance, silica particles dispersed in a polymer matrix, e.g., in SBR composites [2, 38,39]. In our porous Si/PE systems, when the porosity is filled with h-IPA, there is no contrast between the PE and the porosity, and the only contrast remains between the silica and the rest. As such, the scattering profile plotted in Figure 9 corresponds to the scattering of the silica particles (with Si/PE = 4, corresponding to a volume fraction of silica Φ_{Si} = 17%) in a neutron-wise homogeneous matrix. A complex multiscale behavior is observed. At high values of q, information related to primary particles can be extracted, and the scattering associated with the primary particles could be simply fitted with a sphere model (radius R_{Si} = 86.7 Å, polydispersity of 0.2 (for a log-normal distribution). This information is of utmost importance since the same particles have been used in all our systems.

In the membranes, the silica particles are concentrated and have interactions: they form aggregates which contribute to an excess scattering in the low-q region. This scattering can be fitted with a Guinier model [$I(q) = I_0 \exp(-q^2 R_{agg}{}^2/5)$], which gives an approximate radius of the aggregate R_{agg} = 800 Å (with I_0 = 41.4 × 10^3 cm^{-1}) in the case of the initial hydrophilic silica with Si/PE = 4.

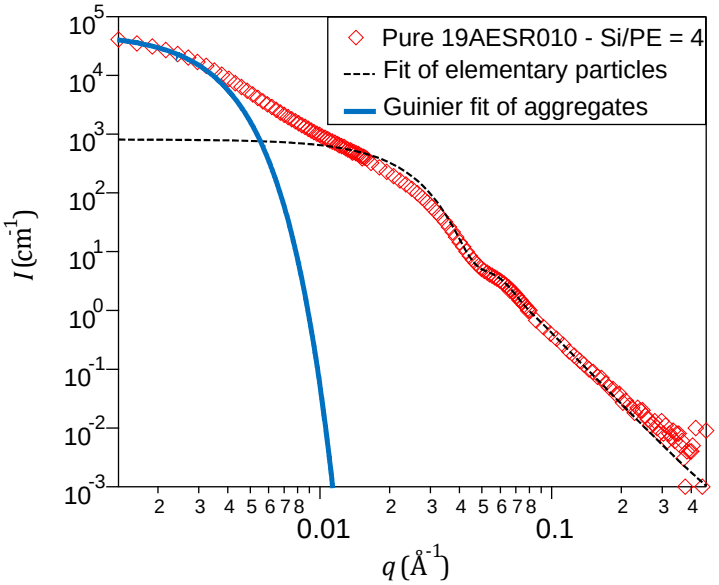

Figure 9: Small angle neutron scattering of a membrane with the initial hydrophilic silica (Si/PE = 4): Absolute intensity I versus wavevector q. The fits at low and high q regions are described in the text.

To further analyze the structure of our systems, we have used the model developed by Baeza et al. [2,40]. In their model, they correlate the information extracted from the elementary particles to that of the aggregates to determine: (i) the distribution of numbers of aggregation N_{agg}, that is to say, the number of elementary particles per aggregate in the membrane and (ii) the compacity of the aggregates κ that is the volume of silica per aggregates relative to the volume of the aggregate. This

method has been used for the membranes containing the initial hydrophilic, grafted hydrophobic and grafted oxidized hydrophilic silica particles with Si/PE = 2.5 (corresponding to Φ_{Si} = 11%). The neutron scattering profiles are plotted in Figure 10.

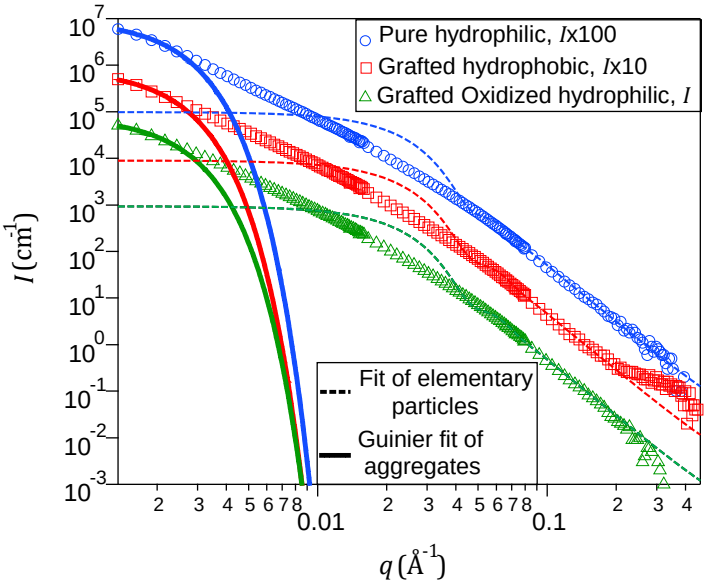

Figure 10: Small angle neutron scattering of membranes with the initial, the grated and the grafted and oxidized silica (Si/PE = 2.5): Absolute intensity I versus wavevector q. Intensities have been multiplied by powers of 10 for clarity. The dotted lines in the high q region is the reported fit of the scattering of the primary particles as determined from Figure 9; the difference with the experimental curves can be attributed to the structure factor. In the low q region, the data have been fitted with a Guinier model.

In these systems, the intensity scattered by the elementary particles is the same as in the more concentrated membranes, although slightly less pronounced. In the low-q region, the scattering is very close from one system to another at the same concentration. The excess scattering due to the presence of aggregates can still be quantified in the low-q region, the values of the Guinier fits are reported in Table 3. The obtained radius of the aggregates R_{agg} and the values of I_0 ($I(q \to 0)$) are very similar, in the ranges 1110 to 1190 Å and 7.8×10^4 to 9.5×10^4 cm^{-1}, respectively. From the determination of the radius of the aggregates R_{agg} and the value of the intensity I_0, the aggregates compacity κ, the average number of aggregation <N_{agg}> and the distribution of numbers of aggregation in the system were determined (see Supporting Information for the detailed procedure). The aggregate compacity (κ) is a crucial factor that links the size of aggregates to the amount of silica they contain, hence characterizing the internal structure of the aggregates and possibly its further wettability. The values of κ and <N_{agg}> are also reported in Table 3 for the three systems. Comparing the compactness and the number of aggregation of samples with aggregates is a direct characterization of the state of dispersion of the samples. For the initial silica, the compacity is evaluated at 50 %; it has to be noted that for the concentrated system Si/PE = 4, the same value of compacity has been obtained. The surface modification tends to slightly decrease the compacity of the aggregates and also decrease the average

number of particles per aggregate, with a better efficacy for the grafted-oxidized sample. In the meantime, the average size of the aggregates is increased for the hydrophobic modification and decreased for a hydrophilic modification. These results tend to indicate that the grafted-oxidized silica dispersion is slightly favored; although the structural variations may seem minor regarding the structure of the silica, it may certainly induce more effect on the formation of the porosity in the matrix and on its wettability conjugated with the surface chemistry.

Table 3: Structure parameters obtained from the neutron scattering data for membranes with silica of different treatments Si/PE = 2.5). I_0 and R_{agg} are obtained from the fits in the low-q region using a Guinier model [$I(q) = I_0 \exp(-q^2 R_{agg}^2/5)$]; the average number of aggregation <N_{agg}> and the compacity of the aggregates κ are obtained following the method given in supporting information

Membrane with silica	I_0 (cm^{-1})	R_{agg} (Å)	<N_{agg}>	κ (%)
Pure hydrophilic	94 990	1163	323	50
Grafted hydrophobic	80 890	1186	307	46
Grafted Oxidized hydrophilic	78 110	1118	278	47

The impact of the surface treatment of silica on the total porosity but, above all, on the porosity accessible to the water in the membranes and the measured resistivity is reported in Figure 11. Moreover, to complete the study, the global electrical resistivity of the membranes was assessed. The ionic conductivity of the separators depends directly on the wettability by the electrolyte. In other words, the increase of water accessible porosity leads to a membrane resistivity decrease [11]. The membranes were characterized using a Palico system. The lowest limit of resistivity is given by the resistivity of the electrolyte itself R_E =1.26 Ω.cm (H_2SO_4 at 27°C, d = 1.28 g.cm^{-3}), measured alone in the Palico cell. The obtained resistivity values are also given in Figure 11 (on a logarithmic scale).

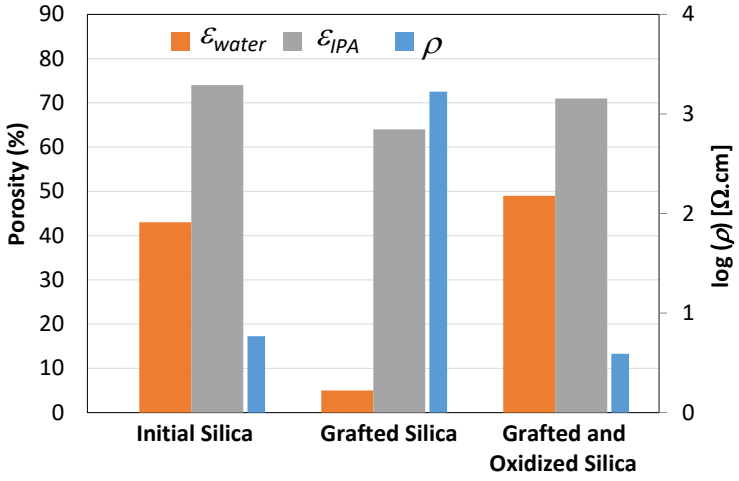

Figure 11: Water accessible Porosity, IPA accessible Porosity and resistivity of the membranes with initial, grafted, and grafted-oxidized silica.

From these data, it is clearly evidenced that the wettability of the membranes is modified with the silica modification. The membranes prepared with initial hydrophilic silica present a water accessible

porosity of 43%. This water accessible porosity decreases drastically to a very low value (5%) for membranes containing hydrophobic grafted silica. Concurrently, the electrical resistivity is increased by much more than 2 decades (precisely from 5.85 ± 0.67 to 1670 ± 440 Ω.cm). As expected and in agreement with the hydrophilicity recovery, the wettability of the membranes elaborated with grafted-oxidized silica is again enhanced, and the measured value of water accessible porosity is 49.5 % while the electrical resistivity (3.9 ± 0.37 Ω.cm) becomes even lower to the value for the membrane with initial silica. A decrease in the total porosity is measured, especially for membranes with grafted silica may be related to a decrease in the oil absorption capacities of grafted silica; still, this value is considered acceptable for this type of conventional recipes (Oil/PE = 7.5 leads on average to a total porosity between 65 – 70 %).

Hence, the used protocol for preparing the silica led to an enhanced electrical conductivity of the membranes, compared to the initial silica. The mechanism can be summarized as follows: using the initial silica, that has a very good hydrophilicity, a low electrical resistivity is obtained. Nevertheless, this silica is constituted of compact aggregates and the silica dispersion is not optimized. One way to improve the dispersion is to pulverize these aggregates by grafting MPTMS. However, if the treatment is stopped at this point, the obtained silica presents a very high hydrophobicity (as shown by the water sorption measurements). It is admittedly much more dispersed in the membrane (as shown by SEM and especially by SANS) but the hydrophobicity leads to a dramatic increase of the electrical resistivity of the membrane. Nevertheless, the oxidation treatment of the grafted silica allows the recovery of a very high hydrophilicity without leading to the compactness of aggregates. This a very important issue because this allows the very good dispersion of the silica in the membrane, even with a slightly higher quality compared to the grafted form as shown by the lower value of aggregates radius for a similar compacity. The resulting porosity accessible to water is increased by a factor 1.15 compared to the membranes with initial silica and the subsequent resistivity is decreased by a factor 1.5.

Conclusion

In this work, the use of chemically modified silica in the membranes has been investigated. The used grafted molecules were tunable hydrophobic molecules that can be chemically modified to obtain hydrophilic tales. The initial silica, the grafted, and the grafted-oxidized silica were processed in membranes formulations. An improvement of the wettability of the separators was recorded for membranes with grafted-oxidized silica compared to the membranes with initial silica. As expected, the porosity in the membranes with only grafted silica was not accessible to water giving a very high electric resistivity.

Furthermore, the structures of these membranes were analyzed by SEM and especially by SANS. The SEM characterization has only shown slight differences between membranes with pure, grafted and the grafted-oxidized silica. In fact, smaller aggregates seemed to be obtained for the latter. Still, these observations were not very reliable for these membranes with a Si/PE ratio of 2.5. That is why SANS experiments were realized on these membranes in contrast-matching experiments (matching PE). These experiments have shown that membranes with grafted silica and with grafted oxidized silica presented smaller aggregates with a lower compacity than those containing the initial silica. Therefore, the combination of a good dispersion and a high hydrophilicity of the grafted-oxidized silica led to very performant membranes for the targeted application of battery separators.

However, some works are still needed to entirely validate this type of membranes for battery applications. First, it is necessary to deeply characterize the mechanical behavior. Nevertheless, it is worth mentioning that the membranes obtained in this work could be handled without any special precautions, suggesting that mechanical properties are not degraded compared to other studied system. The other analysis to be done is the evaluation of the battery performances as the charging and discharging characteristics.

Associated Content

- Supporting Information

The Supporting Information is available free of charge at https://pubs.acs.org/doi/...
1) Energy-dispersive X-ray Spectroscopy (EDX), 2) Analysis of Small Angle Neutron Scattering results

Acknowledgements

The authors gratefully acknowledge Solvay group and ANRT for funding the PhD thesis of Mohammad Abou Taha (CIFRE N 2016/1462), they also acknowledge the European Union Soft Matter Infrastructure EUSMI for funding the SANS experiments at Heinz Maier-Leibnitz Zentrum (MLZ). We want also to acknowledge Christine Lucas from CP2M laboratory for the solid-state NMR analysis. We thank Dr. Paul Sotta (IMP, UMR 5223, Villeurbanne, France) and Dr. Guilhem Baeza (MateIS, UMR 5510, Villeurbanne, France) for the useful discussions. We warmly thank Anne-Caroline Génix (L2C, UMR 5221, Montpellier, France) for the fruitful support regarding SANS data analysis. Finally, we thank Lionel Barriquand (Solvay Silica) for his technical support.

References

1. Courtat, J.; Melis, F.; Taulemesse, J.-M.; Bounor-Legaré, V.; Sonnier, R.; Ferry, L.; Cassagnau, P., Effect of phosphorous-modified silica on the flame retardancy of polypropylene based nanocomposites. *Polym. Degrad. Stab.* **2015**, *119*, 260-274.
2. Baeza, G. P.; Genix, A.-C.; Degrandcourt, C.; Petitjean, L.; Gummel, J. r. m.; Schweins, R.; Couty, M.; Oberdisse, J., Effect of grafting on rheology and structure of a simplified industrial nanocomposite silica/SBR. *Macromolecules* **2013**, *46 (16)*, 6621-6633.
3. Musino, D.; Genix, A.-C.; Chaussée, T.; Guy, L.; Meissner, N.; Kozak, R.; Bizien, T.; Oberdisse, J., Aggregate formation of surface-modified nanoparticles in solvents and polymer nanocomposites. *Langmuir* **2018**, *34 (9)*, 3010-3020.
4. Cassagnau P.; Melis F.; Non-linear viscoelastic behaviour and modulus recovery in silica filled polymers. *Polymer* **2003**, *44*, 6607–6615
5. Cassagnau, P; Melt rheology of organoclay and fumed silica nanocomposites. *Polymer* **2008**, *49*, 2183-2196.
6. Legrand, A.; Hommel, H.; Tuel, A.; Vidal, A.; Balard, H.; Papirer, E.; Levitz, P.; Czernichowski, M.; Erre, R.; Van Damme, H., Hydroxyls of silica powders. *Adv. Colloid Interface Sci.* **1990**, *33 (2-4)*, 91-330.
7. Zhuravlev, L., The surface chemistry of amorphous silica. Zhuravlev model. *Colloids Surf. A* **2000**, *173 (1-3)*, 1-38.
8. Price, P. M.; Clark, J. H.; Macquarrie, D. J., Modified silicas for clean technology. *J. Chem. Soc., Dalton Trans.* **2000**, *(2)*, 101-110.
9. Stein, A.; Melde, B. J.; Schroden, R. C., Hybrid inorganic–organic mesoporous silicates—nanoscopic reactors coming of age. *Adv. Mater.* **2000**, *12 (19)*, 1403-1419.
10. Hair, M.; Hertl, W., Chlorination of silica surfaces. *J. Phys. Chem.* **1973**, *77 (17)*, 2070-2075.
11. Toquet, F.; Guy, L.; Schlegel, B.; Cassagnau, P.; Fulchiron, R., Combined roles of precipitated silica and porosity on electrical properties of battery separators. *Mater. Chem. Phys.* **2019**, *223*, 479-485.
12. Chen, Y. L.; Luo, J. P.; Xu, H.; Hou, X. R.; Gong, M.; Yang, C. S.; Liu, H. C.; Wei, X. Q.; Zhou, L.; Yin, C. Q.; Li, X. M. Core−Shell Structured Polyimide@γ-Al2O3 Nanofiber Separators for Lithium-Ion Batteries. *ACS Appl. Energy Mater.* **2023**, *6*, 1692-1701.
13. Nayanthara, P. S.; Sreenath, S.; Ash, A; Pawar, C.; Dave, V.; Verma, V.; Nagarale, R. K., Robust Polyaniline-silica@polypropylene for High-Performance, High-Capacity Retention All-Vanadium Redox Flow Battery. *ACS Appl. Energy Mater.* **2024**, *7*, 2338−2350.
14. Rao, E.; McVerry, B.; Borenstein, A.; Anderson, M.; Jordan, R. S.; Kaner, R. B. Roll-to-Roll Functionalization of Polyolefin Separators for High-Performance Lithium-Ion Batteries. *ACS Appl. Energy Mater.* **2018**, *1*, 3292−3300.
15. Böhnstedt, W., Aspects of optimizing polyethylene separators. *J. Power Sources* **2001**, *95 (1-2)*, 234-240.
16. Luo, R. P.; Wang, C.; Zhang, Z. X.; Lv W. Q.; Wei, Z. H.; Zhang, Y. N.; Luo, X. Y.; He, W. D. Three-Dimensional Nanoporous Polyethylene-Reinforced PVDF-HFP Separator Enabled by Dual-Solvent Hierarchical Gas Liberation for Ultrahigh-Rate Lithium Ion Batteries. *ACS Appl. Energy Mater.* **2018**, *1*, 921−927.
17. Toquet, F. Study of the combined roles of the Silica/Oil/UHMWPE formulation and process parameters on morphological and electrical properties of battery Separators. *PhD Thesis*, Université Claude Bernard Lyon 1, **2017**.
18. Schmidt, H.; Scholze, H.; Kaiser, A., Principles of hydrolysis and condensation reaction of alkoxysilanes. *J. Non-Cryst. Solids* **1984**, *63 (1-2)*, 1-11.

19. Nishiyama, N.; Horie, K.; Asakura, T., Adsorption behavior of a silane coupling agent onto a colloidal silica surface studied by 29Si NMR spectroscopy. *J. Colloid Interface Sci.* **1989**, *129 (1)*, 113-119.
20. Abou Taha, M.; Bounor-Legaré, V.; de Andrade, F. N.; Lopes do Rosario, R.; McKenna, T. F.; Fulchiron, R., Determination of viscosity average molar masses of polyethylene in a wide range using rheological measurements with a harmless solvent. *Int. J. Polym. Anal. Charact.* **2021**, *26 (7)*, 630-640.
21. Toquet, F.; Guy, L.; Schlegel, B.; Cassagnau, P.; and Fulchiron, R.; Effect of the naphthenic oil and precipitated silica on the crystallization of ultrahigh-molecular-weight polyethylene. *Polymer* **2016**, *97*, 63-68.
22. Morel, F.; Bounor-Legaré, V.; Espuche, E.; Persyn, O.; Lacroix, M., Surface modification of calcium carbonate nanofillers by fluoro-and alkyl-alkoxysilane: Consequences on the morphology, thermal stability and gas barrier properties of polyvinylidene fluoride nanocomposites. *Eur. Polym. J.* **2012**, *48 (5)*, 919-929.
23. Bayse, C. A.; Transition states for cysteine redox processes modeled by DFT and solvent-assisted proton exchange. *Org. Biomol. Chem.* **2011**, *9*, 4748–4751
24. Lloyd, D. R.; Kinzer, K. E.; Tseng, H., Microporous membrane formation via thermally induced phase separation. I. Solid-liquid phase separation. *J. Membr. Sci.* **1990**, *52 (3)*, 239-261.
25. Matsuyama, H.; Kim, M.-m.; Lloyd, D. R., Effect of extraction and drying on the structure of microporous polyethylene membranes prepared via thermally induced phase separation. *J. Membr. Sci.* **2002**, *204 (1-2)*, 413-419.
26. Yoon, J.; Lesser, A. J.; McCarthy, T. J., Locally anisotropic porous materials from polyethylene and crystallizable diluents. *Macromolecules* **2009**, *42 (22)*, 8827-8834.
27. Kim, J.-J.; Hwang, J. R.; Kim, U. Y.; Kim, S. S., Operation parameters of melt spinning of polypropylene hollow fiber membranes. *J. Membr. Sci.* **1995**, *108 (1-2)*, 25-36.
28. Matsuyama, H.; Berghmans, S.; Batarseh, M. T.; Lloyd, D. R., Effects of thermal history on anisotropic and asymmetric membranes formed by thermally induced phase separation. *J. Membr. Sci.* **1998**, *142 (1)*, 27-42.
29. Lin, Y.; Tang, Y.; Ma, H.; Yang, J.; Tian, Y.; Ma, W.; Wang, X., Formation of a bicontinuous structure membrane of polyvinylidene fluoride in diphenyl carbonate diluent via thermally induced phase separation. *J. Appl. Polym. Sci.* **2009**, *114 (3)*, 1523-1528.
30. Rajabzadeh, S.; Maruyama, T.; Sotani, T.; Matsuyama, H., Preparation of PVDF hollow fiber membrane from a ternary polymer/solvent/nonsolvent system via thermally induced phase separation (TIPS) method., *Sep. Purif. Technol.* **2008**, *63 (2)*, 415-423.
31. Kim, J.-K.; Taki, K.; Ohshima, M., Preparation of a unique microporous structure via two step phase separation in the course of drying a ternary polymer solution. *Langmuir* **2007**, *23 (24)*, 12397-12405.
32. Young, T.-H.; Huang, Y.-H.; Chen, L.-Y., Effect of solvent evaporation on the formation of asymmetric and symmetric membranes with crystallizable EVAL polymer. *J. Membr. Sci.* **2000**, *164 (1-2)*, 111-120.
33. Battery Council International, in *BCI Battery Technical Manual*, **2002**, *Section 03B*, pp 3–92.
34. Radulescu, A.; Pipich, V.; Frielinghaus, H.; Appavou, M.-S. In KWS-2, the high intensity/wide Q-range small-angle neutron diffractometer for soft-matter and biology at FRM II, *J. Phys.:Conf. Ser.* **2012**, *351 (1)*, 012026.
35. Glaser, R. H.; Wilkes, G. L.; Bronnimann, C. E., Solid-state 29Si NMR of TEOS-based multifunctional sol-gel materials. *J. Non-Cryst. Solids* **1989**, *113 (1)*, 73-87.
36. Britton, H. T. S., *Conductometric Analysis*. In *Physical Methods in Chemical Analysis Vol 2,* Academic Press Inc. Publishers, New York*,* **1951**, pp 51-104.

37. Yamanaka, J.; Hayashi, Y.; Ise, N.; Yamaguchi, T., Control of the surface charge density of colloidal silica by sodium hydroxide in salt-free and low-salt dispersions. *Phys. Rev. E* **1997**, *55 (3)*, 3028.
38. Ramier, J.; Gauthier, C.; Chazeau, L.; Stelandre, L.; Guy, L., Payne effect in silica-filled styrene–butadiene rubber: Influence of surface treatment. *J. Polym. Sci., Part B:Polym. Phys.* **2007**, *45 (3)*, 286-298.
39. Mélé, P.; Marceau, S.; Brown, D.; de Puydt, Y.; Albérola, N. D., Reinforcement effects in fractal-structure-filled rubber. *Polymer* **2002**, *43 (20)*, 5577-5586.
40. Baeza, G. P.; Genix, A.-C.; Degrandcourt, C.; Petitjean, L.; Gummel, J.; Couty, M.; Oberdisse, J., Multiscale filler structure in simplified industrial nanocomposite silica/SBR systems studied by SAXS and TEM. *Macromolecules* **2013**, *46 (1)*, 317-329.